Suitability Assessment of an Indigenous Heterogeneous Thoracic Phantom for Patient-Specific Quality Assurance in Radiotherapy

Vinod Kumar Gangwar[1,2*], Avinash Agarwal[1], Om Prakash Gurjar[3], Lalit Kumar[4], Vineet Kumar Mishra[2], Surendra Prasad Mishra[5]

1. Department of Physics Bareilly College Bareilly, Uttar Pradesh
2. Medical Physics Division & Radiation Oncology Department, Apollo Medics Hospital, Lucknow
3. Government Cancer Hospital, Mahatma Gandhi Memorial Medical College, Indore
4. Department of Medical Physics, Rajiv Gandhi Cancer Institute and Research Center, New Delhi
5. Department of Radiation Oncology, Dr. Ram Manohar Lohia Institute of Medical sciences, Lucknow, India

A R T I C L E I N F O	A B S T R A C T
	Introduction: Patient-specific quality assurance (PSQA) assumes a vital role in precise and accurate radiation delivery to cancer patients. Since the patient body comprises heterogeneous media, the present study aimed to fabricate a heterogeneous thoracic phantom for PSQA. ***Material and Methods:*** Heterogeneous thoracic (HT) phantom was fabricated using rib cage madeup of bone equivalent material, kailwood to mimic lungs and wax to mimic various body parts. Physical density of all these materials used in phantom fabrication was measured and compared with that of the corresponding part of actual human thorax. One beam was planned on the computed tomography (CT) images of phantom and actual patient thorax region. Dose distribution in both the plans was measured and analyzed. ***Results:*** The estimated densities of heart, lung, ribs, scapula, spine, and chest wall tissues were 0.804±0.007, 0.186±0.010, 1.796±0.061, 2.017±0.026, 2.106±0.029 and 0.739±0.028 respectively in case of HT phantom while 1.038±0.010, 0.199±0.031, 1.715±0.040, 2.006±0.019, 1.929±0.065 and 0.816±0.028 g/cc, respectively in case of actual human thorax region. The depths of isodose curves in HT phantom were also comparable to the isodose curve's depths inreal patient. PSQA results were within ±3% for flat beam (FB) and flattening filtered free beam (FFFB) of 6 megavolts (MV) energy. ***Conclusion:*** Density and dose distribution pattern in HT phantom were similar to that in actual human thorax region. Thus, fabricated HT phantom can be utilized for radiation dosimetry in thoracic cancer patients. The materials used to develop HT phantom are easily available in market at an affordable price and easy to craft.

Introduction

The current era of radiotherapy is a period of rapid evolution in technological advancements. Nowadays, State-of-art technology is capable of delivering accurate and precise radiotherapy (RT) to cancer patients. Modern technology is quite sophisticated due to the involvements of complex hardware and software related to linear accelerators (linac) and treatment planning systems (TPSs). The American Society for Radiation Oncology (ASTRO) illustrated that "nearly two-thirds of all cancer patients receive RT during their disease [1]. Intensity modulation radiation therapy (IMRT), volumetric modulated arc therapy (VMAT), Stereotactic Radio-surgery (SRS) and Stereotactic Body Radiotherapy (SBRT) are the techniques of standard of care of the management of cancer [2].

Intensity modulation of radiation beam, sharp dose gradient around the target and high dose rate treatment delivery mode necessities the need of special concern regarding patient setup reproducibility, advance multi-leaf collimators (MLC) and sophisticated dose computation engines. Interaction of radiation with various heterogeneous tissues including air pockets with widely different radiological properties has a great influence on the dose computation. Precision in dose computation is of paramount importance in the modern RT environment [3].

The task group (TG) 65 of the American Association of Physicists in Medicine (AAPM) inferred that "the overall standard of 3% precision in dose delivery with the relating requirement for better than 2% precision in resolving for inhomogeneities is a sensible [4]. The International Commission on Radiation Units and Measurements (ICRU) has supported general dose accuracy within 5% for better outcomes in RT [5].

The various tumours sites such as head and neck, thorax region, and pelvic region etc. have high inhomogeneities with an organ of widely different

Corresponding Author: Tel: +91-9811187111; Email: gangwarvk@hotmail.com

radiological properties [4]. The dose computation engines always play a crucial role in RT. The dose engine facilitates the accurate absorbed dose in the patient body by considering tissue heterogeneity present in the beam pathway.

It is imperative to verify the radiation dose by delivering the treatment plan on the linac and measuring the dose using the ion chamber (IC) of small volume along with QA phantom, with precision. This helps in verifying the dose computation accuracy and possible flaws in treatment planning. According to AAPM TG 120, the use of different QA phantom of homogenous density equivalent to that of water is quite widespread, since the dose deposition pattern is calculated and verified in phantom of homogeneous density [6]. It is difficult to correlate it with the dose computed in widely heterogeneous tissues of varying densities inside the human body. Therefore, the use of a homogeneous phantom for executing the patient-specific quality assurance (PSQA)in RT may not be justified.

Hence, calculating the dose on computed tomography (CT) images of homogenous QA phantom and measuring it on linac using concerned phantom may not be able to foresee the possible intrinsic limitation of the dose computation engine in encountering the heterogeneous media. Additionally, the uncertainties in the treatment plan, daily setup errors and possible organ motion, misalignment between dosimetric and mechanical components, the physical limitation of hardware used in the treatment unit and various unknown possible errors in the delivery system have vital significance on the treatment outcome. Therefore, a rigorous QA verification is essential to ensure accurate treatment delivery in heterogeneous medium and desired clinical outcomes. A heterogeneous phantom is required to simulate the condition and to ensure the end-to-end validation of treatment delivery in a desired clinical environment. Gurjar *et al.* [7, 8] and Kishore et al.[9] demonstrated the use of tissue-equivalent materials to fabricate the desired phantom.

Though there are few QA phantoms of heterogeneous density (Rando phantom) that are commercially available in the market, these phantoms are not only expansive but have some limitations too i.e. choice of the detector, add-on time and efforts required to evaluate the film/thermoluminescent device (TLD) / Optically stimulated luminescence (OSL), hence, this becomes the limiting factor as far as RT centres in developing countries are a concern. The present study describes the design and fabrication of a low-budget, user-friendly protruding type novel heterogeneous phantom for treatment verification in RT for thoracic cancer patients. This study answers the need to fabricate the heterogeneous density QA phantoms for dose verification in thoracic RT.

Materials and Methods

Phantom design and simulation

A heterogeneous thoracic (HT) phantom was machined to simulate an adult male as illustrated in Figure 1. The HT phantom was comprised of male skeleton bone made of bone equivalent material, kail-wood powder, low-density paraffin-wax, and gel to mimic the rib-case, lung, soft-tissue and heart tissues, respectively. The skeleton was fabricated with the help of a local vendor; paraffin-wax was used to simulate the muscle/fat portion of the body applied around the skeleton with keeping proper space for simulating the lung and heart. Later, kail-wood dust was poured into the space meant to simulate the lungs. An insert of IC of size 0.07ccSemiflex 3D chamber (PTW Freiburg, Germany) was made in HT phantom from neck to end of the lung for measuring the dose at different location points. A UNIDOSE-E electrometer (PTW Freiburg, Germany) along with IC was used for measuring the radiation dose.

The three fiducial lead markers were kept (two at bilateral point and one on anterior point on the HT phantom surface) in the same cross-sectional plane to make three reference points. The CT- machine GE DISCOVERY (GE medical system, WI, USA) was utilized for the CT scan of the HT phantom, with a slice thickness of 0.625 mm. Subsequently, the CT images were imported to the treatment planning system (TPS) Eclipse version 15.5 TPS (Varian Medical System, Palo Alto, Inc., CA, USA). Figure 1 shows the (a) ribs-case, (b) HT-phantom, (c) DRR of the fabricated HT-phantom and (d) setup on the machine.
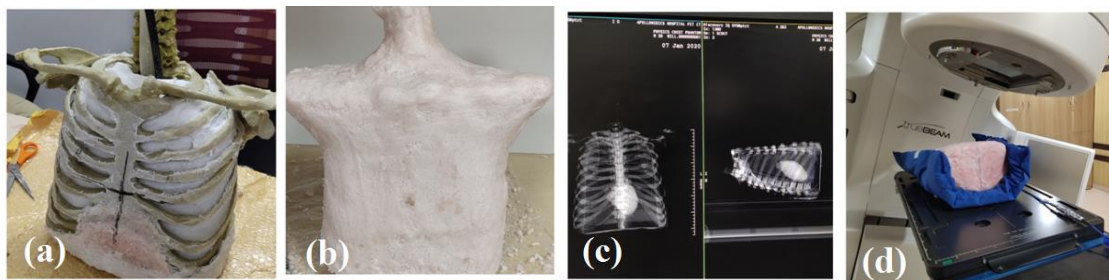

Figure 1. The fabricated (a) ribs-case, (b) HT-phantom, (c) DRR of the fabricated HT-phantom and (d) Phantom setup on the machine along with IC.

Measurements

Density Analysis: The CT images were utilized to determine the Hounsfield-units (HUs) and electron density of the constituent materials used in the fabrication of the HT phantom. The density of all materials used in HT phantom i.e., chest wall, lung, soft tissue, heart etc. was measured with help of the HU tool available in Eclipse TPS.

The density was articulated using the following HU to density conversion relation [10, 11];

$$HU = 1000 \left[(\rho / \rho_{water}) - 1 \right]$$

Where, ρ is the density of the material used and ρ_{water} is the density of the water, respectively.

Analysis of depth of isodose curves: The measurements were executed on the high energy medical linear accelerator True Beam (TB)-SV Clinac (Varian Medical System, Palo Alto, Inc., CA, USA), capable of generating filtered beam (FB) as well as high dose-rate flattening filtered free beam (FFFB). A FB and FFFB of 6 mega-voltage (MV) energies were used for study purpose. These photon energies are most commonly used for treatment in RT [12, 13]. A Source-to-surface distance (SSD) of 100 cm and field size of 10 x 10 cm^2 was used for measurements. A dose calculation grid of 0.25 cm was utilized for the final photon dose calculation. The depth of isodose was compared for different photon energies between HT phantom and CT images of a real patient for the thoracic region. The depth of isodose curves of 100, 95, 90, 85, 80, 70 and 60% were calculated and evaluated for analysis.

PSQA analysis: A cohort of 10 patient cared for lung cancer were retrospectively selected for PSQA analysis using the HT phantom. All the IMRT plans created for 6 MV_FB and 6 MV_FFFB were transferred on the HT phantom and calculated using Eclipse TPS 15.5 Version. The have created the patient specific QA plan same as we creates for daily IMRT treatment patient QA, in this case we selected the HT phantom rather than our Standard QA phantom. The radiation dose was measured using IC and compared (at the point of target deleniation and dose delivery) against Eclipse TPS calculated dose under the same treatment set-up i.e. the point of target deleniation and dose delivery. The IC measured doses were corrected for temperature and pressure deviations. An analytical anisotropic algorithm (AAA) was considered for dose computation.

Results

An HT phantom was fabricated to simulate the thoracic region of the cancer patient. The tissue thickness along the central axis of the photon beam was 3.34 cm of the chest wall, 14 cm of lung and 4.1 cm of soft tissue beyond the lung in fabricated HT phantom. Similar, dimensions were noted for the representative CT images of a real patient, i.e., 3.31 cm of the chest wall, 13 cm of lung and 3.8 cm of soft tissue beyond the lung, respectively. Thus, a phantom of similar size to a real patient was fabricated to mimic the real clinical scenario.

Density measurements

The HU numbers and density pattern for HT phantom and real cancer patient were measured from the CT-images of HT phantom and patient with the help of

$$(HU = 1000 \left[(\rho / \rho_{water}) - 1 \right]$$

Where, ρ is the density of the material used and ρ_{water} is the density of the water, respectively [10,11] and is detailed in Table 1 and Table 2 respectively. The mean HU for heart, lung, ribs, scapula, spine and chest wall tissues were -196.2 ± 6.7, -814.3 ± 10.2, 795.8 ± 61.4, 1017.4 ± 26.1, 1105.7 ± 29.5 and -261.1 ± 28.4 respectively for HT phantom. The mean density for heart, lung, ribs, scapula, spine, and chest wall tissues were 0.804 ± 0.007, 0.186 ± 0.010, 1.796 ± 0.061, 2.017 ± 0.026, 2.106 ± 0.029 and 0.739 ± 0.028 g/cc, respectively for HT phantom. Additionally, the mean HU for heart, lung, ribs, scapula, spine, and chest wall tissues were 38.3 ± 9.7, -800.8 ± 31.4, 715.4 ± 39.9, 1005.6 ± 19.3, 929.0 ± 64.6 and -184.41 ± 27.6 respectively, for real cancer patient.

Table 1. The Hounsfield units (HUs) and density of the material used for fabrication of HT- phantom.

Measurements Points	HU Numbers						Density (g/cc)					
	Heart	Lung	Ribs	Scapula	Spine	Chest wall	Heart	Lung	Ribs	Scapula	Spine	Chest wall
1	-194	-826	710	1031	1090	-309	0.806	0.174	1.710	2.031	2.090	0.691
2	-198	-815	711	1010	1050	-272	0.802	0.185	1.711	2.010	2.050	0.728
3	-200	-828	790	1026	1078	-241	0.800	0.172	1.790	2.026	2.078	0.759
4	-210	-802	781	1002	1121	-227	0.790	0.198	1.781	2.002	2.121	0.773
5	-195	-795	835	998	1103	-232	0.805	0.205	1.835	1.998	2.103	0.768
6	-190	-811	850	979	1129	-290	0.810	0.189	1.850	1.979	2.129	0.710
7	-203	-818	770	1032	1105	-278	0.797	0.182	1.770	2.032	2.105	0.722
8	-188	-822	760	1075	1119	-231	0.812	0.178	1.760	2.075	2.119	0.769
9	-193	-812	871	1018	1158	-279	0.807	0.188	1.871	2.018	2.158	0.721
10	-191	-814	880	1003	1104	-252	0.809	0.186	1.880	2.003	2.104	0.748
Mean	-196.2	-814.3	795.8	1017.4	1105.7	-261.1	0.804	0.186	1.796	2.017	2.106	0.739
SD	6.7	10.2	61.4	26.1	29.5	28.4	0.007	0.010	0.061	0.026	0.029	0.028

Table 2. The Hounsfield units (HUs) and density of the material used for fabrication of a real cancer patient.

| Measurements Points	HU Numbers						Density (g/cc)					
	Heart	Lung	Ribs	Scapula	Spine	Chest wall	Heart	Lung	Ribs	Scapula	Spine	Chest wall
1	44	-816	762	1009	850	-145	1.044	0.184	1.762	2.009	1.850	0.855
2	37	-802	780	990	910	-180	1.037	0.198	1.780	1.990	1.910	0.820
3	39	-835	715	985	885	-165	1.039	0.165	1.715	1.985	1.885	0.835
4	33	-810	708	1015	950	-205	1.033	0.190	1.708	2.015	1.950	0.795
5	30	-773	685	1007	887	-215	1.030	0.227	1.685	2.007	1.887	0.785
6	34	-754	680	975	980	-225	1.034	0.246	1.680	1.975	1.980	0.775
7	50	-802	682	1005	860	-187	1.050	0.198	1.682	2.005	1.860	0.813
8	57	-757	699	1002	920	-185	1.057	0.243	1.699	2.002	1.920	0.815
9	35	-850	675	1037	1050	-195	1.035	0.150	1.675	2.037	2.050	0.805
10	24	-809	768	1031	998	-142	1.024	0.191	1.768	2.031	1.998	0.858
Mean	38.3	-800.8	715.4	1005.6	929.0	-184.4	1.038	0.199	1.715	2.006	1.929	0.816
SD	9.7	31.4	39.9	19.3	64.6	27.6	0.010	0.031	0.040	0.019	0.065	0.028
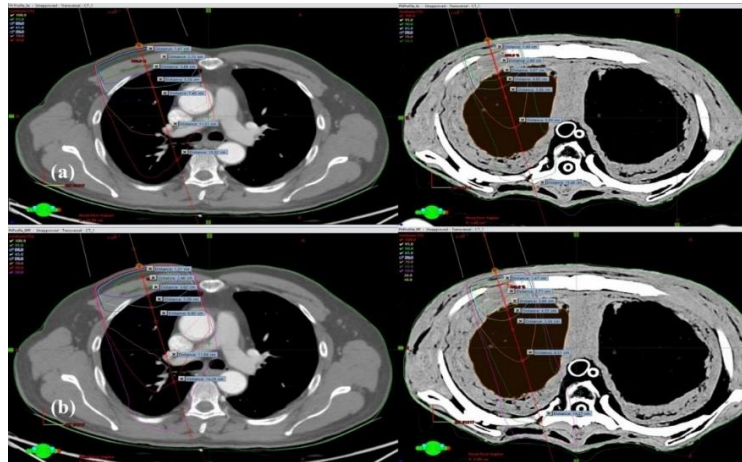
Figure 2. The depth dose analysis for (a) 6 MV_FB and (b) 6 MV_FFFB on the CT-images of HT phantom and real cancer patient.

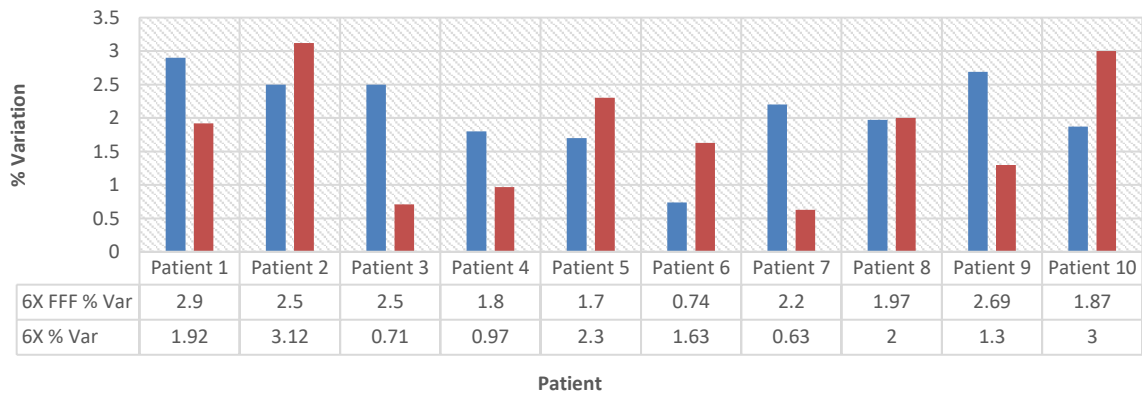|	Patient 1	Patient 2	Patient 3	Patient 4	Patient 5	Patient 6	Patient 7	Patient 8	Patient 9	Patient 10
6X FFF % Var	2.9	2.5	2.5	1.8	1.7	0.74	2.2	1.97	2.69	1.87
6X % Var	1.92	3.12	0.71	0.97	2.3	1.63	0.63	2	1.3	3

Figure 3. Graph illustrates of the deviation of data between the IC measured dose and TPS calculated dose.

The mean density for heart, lung, ribs, scapula, spine, and chest wall tissues were 1.038 ± 0.010, 0.199 ± 0.031, 1.715 ± 0.040, 2.006 ± 0.019, 1.929 ± 0.065 and 0.816 ± 0.028 g/cc, respectively for the real cancer patient. The detailed HU numbers and density pattern data and variation for HT phantom and real cancer patient is represented in the table and it shows phatom is quite suitable for the use.

Analysis of depth of isodose curves

Depth of isodose profiles for 6 MV_FB and 6 MV_FFFB on the CT images of HT phantom and real cancer patient were analyzed and detailed in Table3.The isodose curves are shown in figure 2 (a) 6MV_FB and figure 2 (b) 6 MV_FFFB on the CT images of the HT phantom and real cancer patients, respectively.

Table 3.Isodose depth analysis for6 MV_FB and 6 MV_FFFB on the CT-images of HT phantom and real cancer patient.

Isodose lines(in %)	Depth of isodose lines for 6MV_FB(in cm)		Depth of isodose lines for 6 MV_FFFB(in cm)	
	Patient	HT Phantom	Patient	HT Phantom
100	1.47	1.50	1.37	1.47
95	2.72	2.90	2.48	2.71
90	3.86	3.88	3.60	3.66
85	5.56	4.80	5.09	4.55
80	7.40	5.88	6.80	5.56
70	11.51	9.00	11.04	8.51
60	15.32	15.48	14.26	14.27

The depth of the 100, 95 and 90 % isodose curves were comparable for both photon beams on the CT-images of HT phantom and real cancer patient, respectively. Additionally, there was a noticeable difference between the depth of isodose curves of 85, 80 and 70 % for both photon beams on the CT images of HT phantom and real cancer patient, respectively. The difference in the depth of the above isodose can be explained using the fact that lung density varies in real patient depending upon the respiratory phase and were different from the density of kail-wood dust. This leads to the different attenuation of the photon beam in real lung and kail-wood dust.

PSQA analysis

Figure 3 illustrates the deviations between IC measured and Eclipse TPS calculated radiation dose for ten patients. The mean deviations were 2.1± 0.6 % and 1.7 ± 0.8 % for 6 MV_FB and 6 MV_FFFB beam respectively.

Discussion

In this modern technology era with greater capabilities of particle simulation in heterogeneous media, the accuracy of dose calculation algorithms has been improved over time. Though, patient-specific QA is a mandatory task to be performed before delivering the radiation dose to the cancer patient in a modern clinic. PSQA warrants that the delivered dose and planned dose (TPS calculated) are within the prescribed tolerance limits of ± 3% [5].

The study was carried out to fabricate an HT phantom to mimic the thoracic region of a cancer patient. Further, the study tried to differentiate the change in photon dose distribution to density variations (chest wall, ribs-case, lung and soft-tissue) in the thoracic region of the cancer patient. The physical dimensions of the HT phantom were comparable to the dimension of the CT images of the real cancer patient. The estimated densities of materials used to mimic the heart, lung, ribs, scapula, spine, and chest wall tissues were 0.804 ± 0.007, 0.186 ± 0.010, 1.796 ± 0.061, 2.017 ± 0.026, 2.106 ± 0.029 and 0.739 ± 0.028 respectively for HT phantom. These densities values were comparable to the densities estimated from the heart, lung, ribs, scapula, spine and chest wall tissues of the real patient i.e., 1.038 ± 0.010, 0.199 ± 0.031, 1.715 ± 0.040, 2.006 ± 0.019, 1.929 ± 0.065 and 0.816 ± 0.028

g/cc, respectively. The depths of isodose curves in HT phantom were also comparable to the isodose curve's depths in a real patient. The PSQA analysis reveals that HT phantom shows good congruence with TPS calculations (i.e., ± 3 %) for both photon energies. Therefore, HT phantom can mimic the thoracic region of the human body and can be utilized for radiation dosimetry in thoracic cancer patients. The materials used to develop HT phantom are easily available in the market at an affordable price and easy to craft.

Gurjar *et al.*, reported kail-wood and pine-wood in a combination of polystyrene to simulate the heterogeneous chest phantom for PSQA [7,8]. Singh *et al.* also simulated their indigenously developed pelvic phantom made of different materials including wax material and bone equivalent material and found the density pattern equivalent to their corresponding parts of the pelvic region [14], the same bone material has been used in the current study. Additionally, Kumar *et al.* [15, 16] detailed the development of a heterogeneous phantom for lung cancer PSQA using the combination of recemosa wood/dust and Poly (methyl methacrylate). Gurjar *et al.* [7, 8] and Kumar et al. [15, 16] demonstrated the use of kail-wood/pine-wood and racemosa-wood and their dust to mimic the lung tissue but didn't develop an actual phantom of human body shape. Our study has an edge to develop a heterogeneous phantom of the actual size and shape of the human body. With the advent of technology, researchers had reported the three-dimensional (3D) polyjet printing and fused deposition modelling (FDM) techniques to construct the personalized phantoms for dose verification[17, 18].No exanimate phantom can mimic all the highlights of a living patient. The prime objective of fabricating a phantom is to develop a phantom that integrates the fundamental highlights of the patient. A phantom can examine, validate and guide radiation delivery in a controlled environment.

In the modern era, most of the centres in developing countries are using traditional methods of PSQA such as slab phantom of uniform density 30×30×30 cm³ for PSQA. Owing to the uniform density of the slab phantom, it is very easy to achieve the tolerance limit of ± 3% between TPS calculation and PSQA result as prescribed by the ICRU report 83[4,9,10]. Though, the patient body is thoroughly heterogeneous so it may not

be useful to perform PSQA with homogenous slab phantom in the era of highly beam modulated technique like IMRT, VMAT and SBRT. Although, there are heterogeneous phantoms available namely viz., IMRT thorax CIRS 002LFC [19] and ATOM® phantom [20] (CIRS tissue simulation & phantom technology, Asbury Ave Norflok, VA), hospitals in developing nations may not beable to purchase and use them because of the high cost.

Hence, based on the densities estimated for bone, kail-wood and paraffin-wax, it can culminate that these materials can be used to fabricate a thoracic phantom. The comparable depth of isodose curves and PSQA results warrants that fabricated phantom can be utilized for quality assurance program in radiotherapy.

Conclusion

The present study fabricates a heterogeneous thoracic phantom and results affirm the similarities between its density pattern and that of the real patient thoracic region. Dose distribution pattern in CT images of both the media via HT phantom and that of the actual patient thoracic region also similar. The materials used for the fabrication of thoracic phantom were locally available, strong enough to sustain structural integrity and easy to craft. Further, it is easy to use and the cost of fabricating the phantom is minimal compare to its counterparts. Therefore, the HT phantom can be prepared locally and can be used for PSQA.

Acknowledgment

References

1. Shaverdian N, Yeboa DN, Gardner L, Harari PM, Liao K, McCloskey S, et al. Nationwide survey of patients′ perspectives regarding their radiation and multidisciplinary cancer treatment experiences. J OncolPract 2019;15(12):e1010 7.
2. Kumar L, Kishore V, Bhusan M, Yadav G, Dewan A, Kumar P, et al. Impact of flatting filter free photon beam on RapidArc radiotherapy for Gynaecological malignancies: A comparative study. Iran J Med Phys.2021;18(1):23-9.
3. Xing L, Curran B, Hill R, Holmes T, Ma L, Forster KM, et al. Dosimetric verification of a commercial inverse treatment planning system. Phys Med Biol 1999; 44(2):463-78.
4. Papanikolau N, Battista JJ, Boyer AL, Kappas C, Klein E, et al. Tissue Inhomogeneity Corrections for Megavoltage Photon Beams. Report of Task Group No. 65 of the Radiation Therapy Committee of the American Association of Physicist in Medicine. AAPM Report No. 85;2004.
5. ICRU report 83. Prescribing, recording, and reporting photon-beam intensity-modulation radiation therapy (IMRT). In: International Commission on Radiation Units and Measurements, Bethesda.
6. Low DA, Moran JM, Dempsey JF, Dong L, Oldham M. Dosimetry tools and techniques for IMRT. Med Phys. 2011; 38(3):1313-38.
7. Gurjar OP, Mishra PK, Singh N, Bagdare P, Mishra SP. Dosimetric study for the development of heterogeneous chest phantom for the purpose of patient-specific quality assurance. RadiatProt Environ. 2015;38(4):139-43
8. Gurjar OP, Paliwal RK, Mishra SP. A dosimetric study on slabpinewood-slab phantom for developing the heterogeneous chest phantom mimicking actual human chest. J Med Phys. 2017; 42(2):80-5.
9. Kishore V, Kumar L, Yadav G, Bhusham M. A study for the development of a low density heterogeneous phantom for dose verification in high energy photon beam. j.radphyschem.2020;170:108638
10. Gurjar OP, Mishra SP, Bhandari V, Pathak P, Patel P, Shrivastav G. Radiation dose verification using real tissue phantom in modernradiotherapy techniques. J Med Phys 2014;39(1):44-9.
11. Kumar L, Kishore V, Bhushan M, Dewan A, Yadav G, Raman K, et al. Impact of Acuros XB algorithm in deep inspiration breath hold (DIBH) respiratory techniques used for the treatment of left breast cancer. Rep PractOncolRadiother. 2020;25(4):507 14.
12. Kumar L, Yadav G, Raman K, Bhushan M, Pal M. The dosimetric impact of different photon beam energy on RapidArc radiotherapy planning for cervix carcinoma. J Med Phys. 2015; 40(4):207-13.
13. Kumar L, Yadav G, Samuvel KR, Bhushan M, Kumar P, Suhail M, Pal M. Dosimetric influence of filtered and flattening filter free photon beam on rapid arc (RA) radiotherapy planning in case of cervix carcinoma. Rep PractOncolRadiother. 2017;22(1):10-8.
14. Singh S, Raina P, Gurjar OP. Dosimetric Study of an Indigenous and Heterogeneous Pelvic Phantom for Radiotherapy Quality Assurance.Iran J Med Phys. 2020;17(2):120-5
15. Kumar L, Yadav G, Kishore V, Bhushan M. Dosimetric validation of Acuros XB photon dose calculation algorithm on an indigenously fabricated low density heterogeneous phantom. RadiatProt Environ 2019; 42(4):173-9.
16. Kumar L, Kishore V, Bhushan M, Kumar P, Kumar G. Design and fabrication of a thoracic phantom for radiation dose verification in megavoltage X-ray beam, Materials Today: Proceedings,2022; 49: 3050-5.
17. Zhang F, Zhang H, Zhao H, He Z, Shi L, He Y, et al. Design and fabrication of a personalized anthropomorphic phantom using 3D printing and tissue equivalent materials. Quant Imaging Med Surg 2019;9(1):94-100.
18. Mayer R, Liacouras P, Thomas A, Kang M, Lin L, Simone CB 2nd. 3D printer generated thorax phantom with mobile tumor for radiation dosimetry. Rev SciInstrum. 2015; 86(7):074301.
19. CIRS tissue simulation & phantom technology, Asbury Ave Norflok, VA. Available from https://www.cirsinc.com/products/radiation-therapy/imrt-thorax-phantom/ [last accessed on September 15, 2020]
20. CIRS tissue simulation & phantom technology, Available from https://www.cirsinc.com/products/radiation-therapy/atom-dosimetry-verification phantoms/ [last accessed on September 15, 2020]